Electronic Supplementary Material (ESI) for RSC Advances.

Electronic Supporting Information (ESI)

Asymmetry-unit-dominated double slow-relaxation modes of 2, 6-dimethyl-3, 5-heptanedione dysprosium SMMs

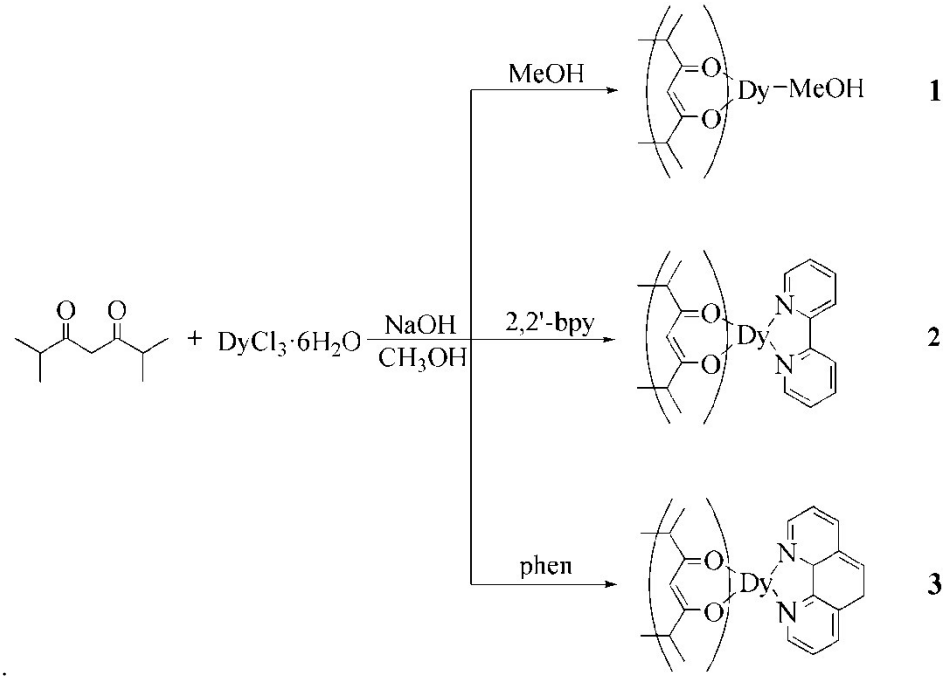

Scheme S1. Synthesis of complexes **1**−**3**

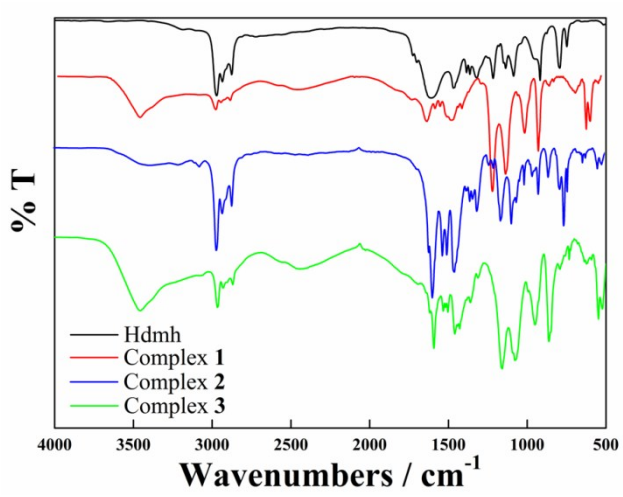

Fig. S1 IR spectra of Hdmh and complexes **1**−**3**

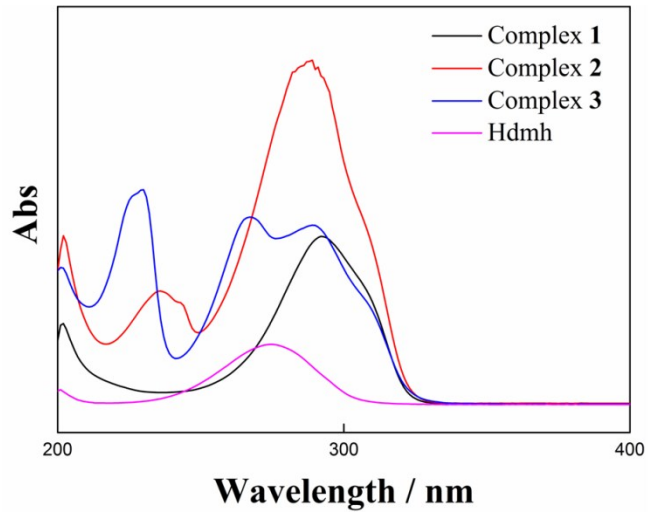

Fig. S2 UV absorption spectra Hdmh and complexes **1**−**3**

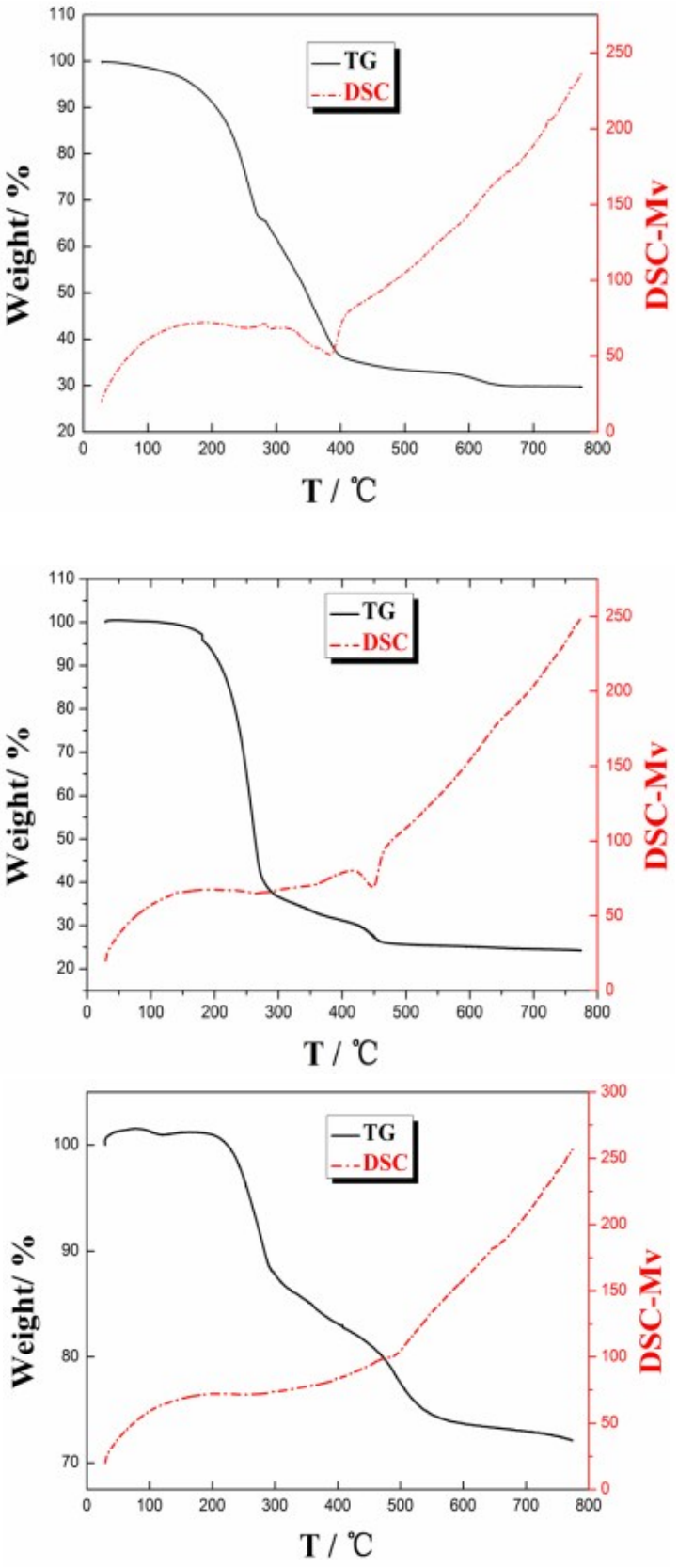

Fig. S3 TG-DSC curves of complexes **1**−**3**

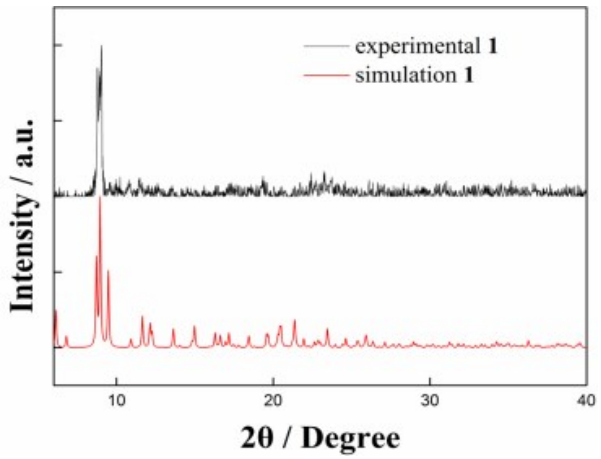

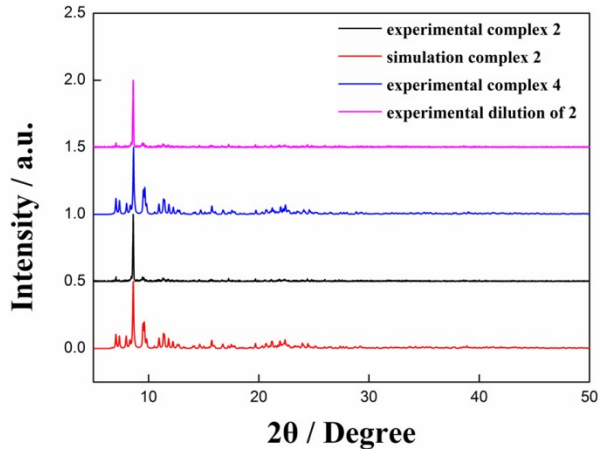

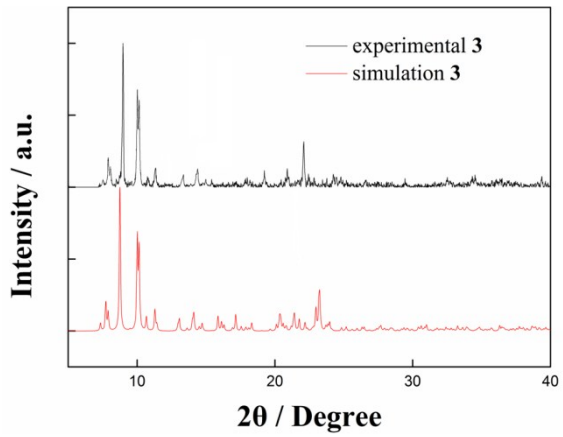

Fig. S4 Powder X-ray diffraction of complexes **1**−**3**

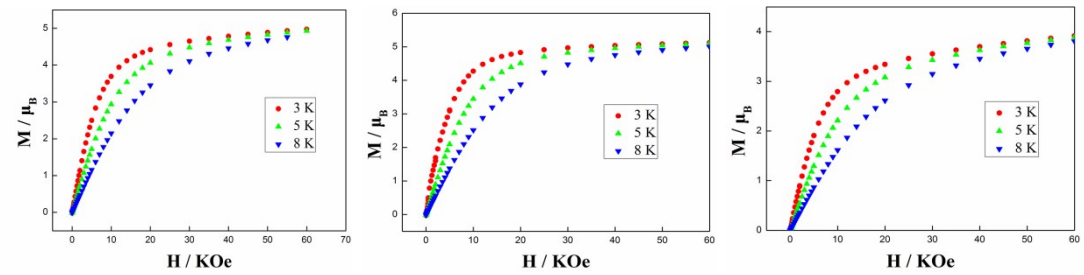

Fig. S5 *M vs H* data for complexes **1** (left), **2** (middle) and **3** (right) at temperature range of 3−8 K

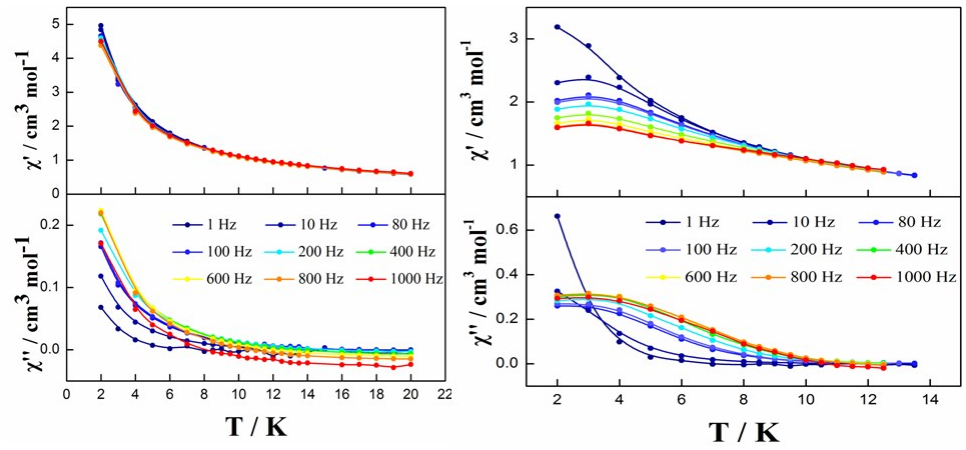

Fig. S6 Temperature dependence of the in-phase (χ') and out-of-phase (χ'') ac susceptibility of complex **1** under 0 Oe (left) and 2000 Oe(right).

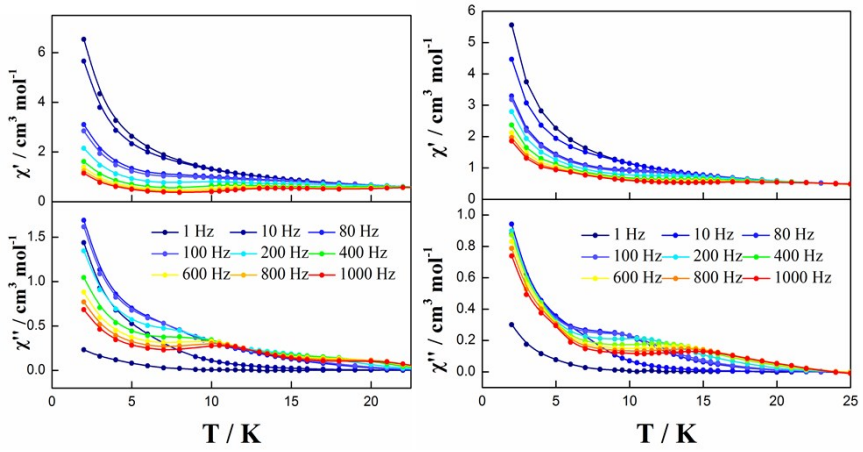

Fig. S7 Temperature dependence of the in-phase (χ') and out-of-phase (χ'') ac susceptibility of complex **2** (left) and **3** (right) under 0 Oe.

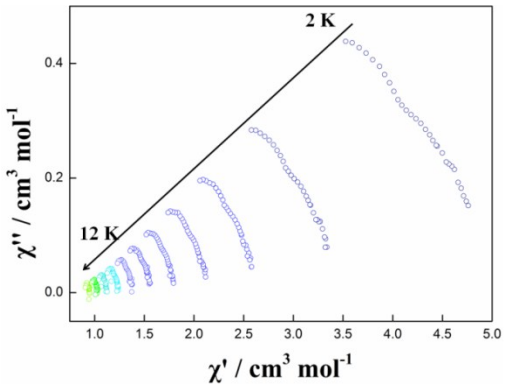

Fig. S8 Cole-Cole plots measured in the temperature range of 2.0−12.0 K under 0 Oe for complex **1**, one line represents 1 K.

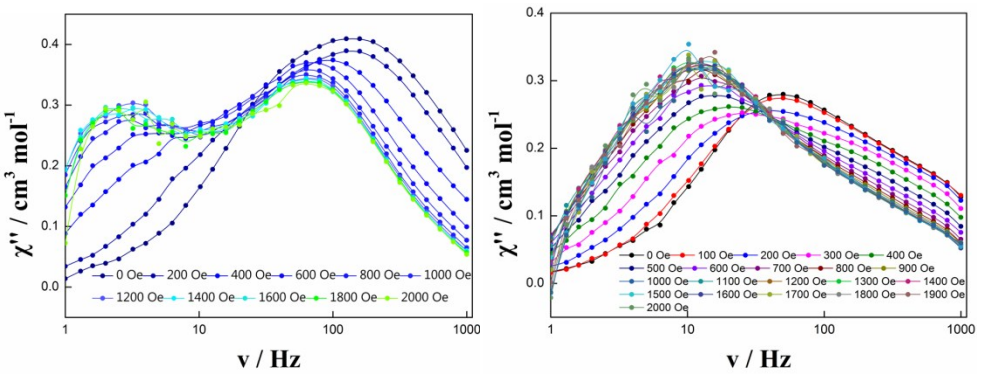

Fig. S9 Frequency dependence of the imaginary (χ”) parts of the ac susceptibility at 8 K and 5 K with different ac frequency between 1 and 1000 Hz and different dc-field in the range of 0−2000 Oe for complex **2** (left) and complex **3** (right), respectively.

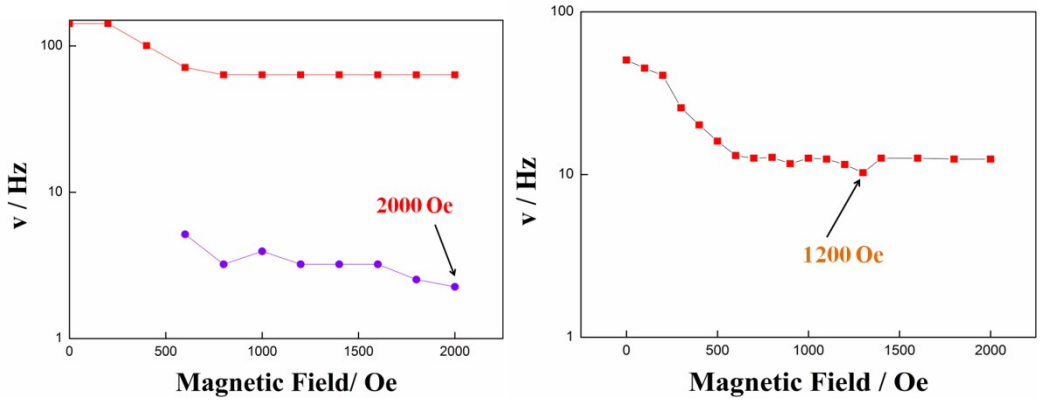

Fig. S10 Selected Optimizing DC field for complex **2** (left) and complex **3** (right), respectively.

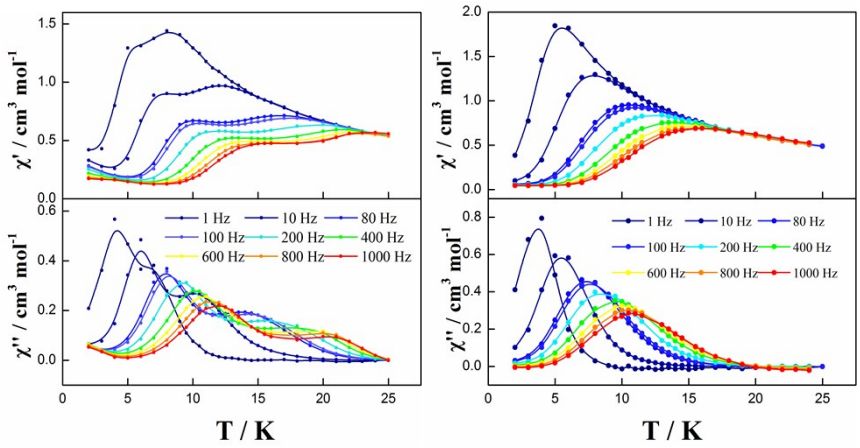

Fig. S11 Temperature dependence of the in-phase (χ') and out-of-phase (χ'') ac susceptibility of complex **2** and **3** under 2000 field (left) and 1200 field (right).

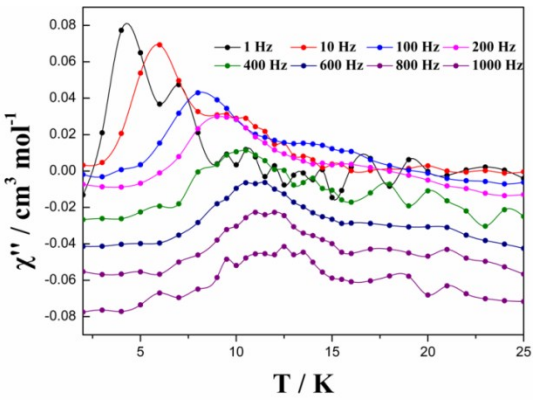

Fig. S12 Temperature dependence of the out-of-phase (χ'') ac susceptibility by 1:20 Lu diluted for complex **2** under 2000 Oe.

Table S1. Selected bond lengths and angles for complexes **1**−**3**

1		**2-Dy1**		**2-Dy2**		**3**	
Dy(1)-O(1)	2.268(7)	Dy(1)-O(1)	2.361(6)	Dy(2)-O(7)	2.299(6)	Dy(1)-O(1)	2.291(3)
Dy(1)-O(2)	2.279(8)	Dy(1)-O(2)	2.318(6)	Dy(2)-O(8)	2.341(6)	Dy(1)-O(2)	2.302(3)
Dy(1)-O(3)	2.279(6)	Dy(1)-O(3)	2.326(6)	Dy(2)-O(9)	2.304(6)	Dy(1)-O(3)	2.312(3)
Dy(1)-O(4)	2.256(7)	Dy(1)-O(4)	2.306(7)	Dy(2)-O(10)	2.336(7)	Dy(1)-O(4)	2.327(3)
Dy(1)-O(5)	2.243(9)	Dy(1)-O(5)	2.312(6)	Dy(2)-O(11)	2.296(6)	Dy(1)-O(5)	2.328(3)
Dy(1)-O(6)	2.341(7)	Dy(1)-O(6)	2.316(6)	Dy(2)-O(12)	2.291(6)	Dy(1)-O(6)	2.310(3)
Dy(1)-O(7)	2.381(5)	Dy(1)-N(3)	2.597(7)	Dy(2)-N(1)	2.599(7)	Dy(1)-N(1)	2.582(4)
		Dy(1)-N(4)	2.582(7)	Dy(2)-N(2)	2.582(7)	Dy(1)-N(2)	2.575(4)

Table S2. Shape analysis of complex **1** using SHAPE 2.1 software

Complex	Pentagonal bipyramid	Capped octahedron	Capped trigonal prism
1	4.745	2.040	0.853

Table S3. α, φ angle (°) and shape analysis of complexes **2** and **3** using SHAPE 2.1 software

Complexes	Square antiprism (D_{4d})	Triangular dodecahedron (D_{2d})	Biaugmented trigonal prismatic (C_{2v})	α angle (°)	φ angle (°)
2 (Dy1(III) ion)	0.551	2.348	1.974	56.95	45.76
2 (Dy2(III) ion)	0.573	2.048	2.265	56.95	43.67
3 (Dy(III) ion)	0.468	2.539	2.751	54.94	45.76

Table S4. Fitted parameters of the Cole-Cole plots for complex **2** at *H*dc = 0 Oe

T / K	χ_S	χ_T	τ	α
2	0.84815	6.28850	0.00293	0.31534
3	0.64529	4.16232	0.00224	0.30131
4	0.50400	3.13340	0.00216	0.30052
5	0.41803	2.52562	0.00203	0.29612
6	0.36150	2.10889	0.00176	0.28026
7	0.30826	1.80774	0.00137	0.27116
8	0.26128	1.58083	0.00100	0.27301
9	0.22132	1.40813	0.00070	0.29057
10	0.21715	1.26906	0.00052	0.30321
11	0.25881	1.15396	0.00044	0.29840
12	0.33078	1.05658	0.00044	0.26881

Table S5. Fitted parameters of the Cole-Cole plots for complex **3** at *H*dc = 0 Oe

T / K	χ_S (total)	$\Delta\chi_1$	τ_1	α_1	$\Delta\chi_2$	τ_2	α_2
2	1.18388	2.37339	0.01199	0.21376	2.10741	0.00038	0.24067
3	0.72590	1.26282	0.01207	0.15630	1.77759	0.00041	0.34551
4	0.57927	0.94469	0.01062	0.15326	1.30439	0.00036	0.34830
5	0.49207	0.71933	0.00880	0.12760	1.05487	0.00028	0.41600
6	0.64870	0.51998	0.00665	0.06735	0.56800	0.00056	0.32052
7	0.61250	0.44224	0.00508	0.03008	0.45016	0.00056	0.26424
8	0.55673	0.33968	0.00307	0.01146	0.36053	0.00056	0.23663
9	0.53278	0.27558	0.00235	0.28276E-06	0.32311	0.00055	0.17491
10	0.51064	0.18715	0.00193	0.43932E-06	0.33243	0.00058	0.13374
11	0.48990	0.12458	0.00177	0.21591E-06	0.33170	0.00051	0.08716
12	0.47563	0.10327	0.00150	0.27310E-06	0.29346	0.00041	0.05023

Table S6. Fitted parameters of the Cole-Cole plots for complex **2** at *H*dc = 2000 Oe

T / K	χ_S (total)	$\Delta\chi_1$	τ_1	α_1	$\Delta\chi_2$	τ_2	α_2
7	0.10228	1.16726	0.03579	0.35740	0.32732	0.01131	0.1177E-07
8	0.10504	1.22120	0.07435	0.43197	0.47584	0.00371	0.9581E-16
9	0.13900	0.88253	0.08238	0.21353	0.65876	0.00191	0.2680E-18
10	0.13964	0.72970	0.03784	0.15946	0.59111	0.00097	0.8178E-18
11	0.14661	0.62750	0.01916	0.13328	0.52260	0.00054	0.1923E-17
12	0.16061	0.55482	0.01073	0.11467	0.45689	0.00033	0.4915E-17
13	0.18174	0.48979	0.00667	0.08329	0.40318	0.00022	0.9506E-17
14	0.22367	0.45047	0.00414	0.08555	0.32090	0.00015	0.1387E-16
15	0.26712	0.40683	0.00273	0.06656	0.25082	0.00012	0.1078E-16
16	0.31504	0.36945	0.00185	0.05470	0.17901	0.00010	0.1446E-16

Table S7. Fitted parameters of the Cole-Cole plots for complex **3** at *H*dc = 1200 Oe

T / K	χ_S	χ_T	τ	α
2	0.54334	2.18871	0.05954	0.43781
3	0.54234	1.88452	0.02895	0.36662
4	0.52693	1.70407	0.01737	0.32727
5	0.51347	1.56381	0.01128	0.29426
6	0.48867	1.36222	0.00558	0.24853
7	0.46346	1.21835	0.00309	0.22409
8	0.44349	1.10306	0.00187	0.20622
9	0.42784	1.01031	0.00118	0.20039
10	0.41353	0.93461	0.00078	0.20161
11	0.41468	0.86843	0.00054	0.20262
12	0.39248	0.78324	0.00036	0.20004

Table S8. Parameters used to fit the Arrhenius plots from Fig. 4 using approximations $1/\tau = CT^n + \tau_0^{-1}\exp(-U_{eff}/k_BT)$

Optimum dc field	Complex **2-1**	Complex **2-2**	Complex **3**
$C/s^{-1}k^{-n}$	0.22	1.10	3.40
n	3.61	5.58	7.64
τ_0/s	1.87×10^{-6}	6.60×10^{-6}	2.49×10^{-6}
U/K	91.76	62.84	73.69